Energy 189 (2019) 116149

Contents lists available at ScienceDirect

Energy

journal homepage: www.elsevier.com/locate/energy

Optimizing wind farm layout by addressing energy-variance trade-off: A single-objective optimization approach

Longyan Wang [a, b, c], Ming J. Zuo [c, *], Jian Xu [a], Yunkai Zhou [a], Andy C. Tan [d]

[a] Research Centre of Fluid Machinery Engineering and Technology, Jiangsu University, Zhenjiang, 212013, Jiangsu Province, China
[b] Institute of Fluid Engineering Equipment, JITRI, Jiangsu University, Zhenjiang, 212013, Jiangsu Province, China
[c] Department of Mechanical Engineering, University of Alberta, Edmonton, AB T6G 1H9, Canada
[d] LKC Faculty of Engineering & Science, Universiti Tunku Abdul Rahman, Bandar Sungai Long, Cheras, 43000, Kajang, Selangor, Malaysia

ARTICLE INFO

Article history:
Received 7 May 2019
Received in revised form
19 August 2019
Accepted 16 September 2019
Available online 24 September 2019

Keywords:
Wind farm layout
Wind power variability
Weighted optimization
Confidence interval optimization
Monte Carlo method

ABSTRACT

Wind farm layout optimization results depend on the optimization objectives, such as power output and variance. This paper investigates an alternative strategy for wind farm layout optimization by trading off the mean wind power output and power variance. Two optimization schemes, the weighted optimization and confidence interval optimization are compared in term of their performances on trading off energy-variance. For the weighted optimization, the objective function weight value α varies from 0 to 1 (implying the optimization objective shifts its weight from the power variance to the power output), while for the confidence interval (CI) optimization, either the lower or the upper limit of power output CI is maximized/minimized. It is found that the CI maximization achieves a trade-off of mean power output and power variance similar to the weighted optimization with $\alpha \geq 0.6$, and the same individual power output range (192 kW–207 kW) is obtained with staggered placements of wind turbines. The CI minimization obtains a trade-off of average power output and power variance close to the weighted optimization with $\alpha \leq 0.4$, and the optimal wind turbine locations are aligned. The advantage of CI optimization lies on its capability of predicting the power output uncertainty.

1. Introduction

Given the severe environmental impacts caused by traditional fossil fuel exhaust, research on renewable energy which serves as an alternative to generating electricity has been an emerging hot topic in industry and academic research in recent years [1]. Among the different types of renewable energies, such as solar power, hydro power, tidal power, and geothermal power, wind power has been reported to have the most significant growth in the last decade [2]. In 2015, the wind energy accounted for 4.7% of total electricity generation in United States, and the share of electrical power yield from wind energy is targeted to be 20% by 2030 [3,4]. The wind energy is captured by placing wind turbines in cluster for the purpose of exploiting the local wind power as much as possible [5]. However, the wake interaction of downstream turbines emerges as a major problem for exploiting wind energy when wind turbines are clustered in a wind farm [6]. The adverse effect of wake interactions includes reduction of power output and increases of fatigue load of wind turbine components [7]. In order to mitigate the wake interactions between wind turbines, wind farm layout optimization and placement of turbines play a key role to optimize power output from the wind farm [8,9].

The wind farm layout optimization problem was first studied by Mosetti et al. [10] to optimize layout design of turbines in order to maximize its average power output. Different wind conditions with discrete variations in wind speed/direction were studied and the average power output increase compared to the random wind farm layouts after optimization for all wind conditions. In order to provide a more realistic assessment of wind properties of a given region, a more complex wind condition (joint distribution of wind speed-direction) is employed for the wind farm layout optimization study in Ref. [11]. The wind farm design under joint distribution of wind speed and wind direction is also investigated in Ref. [12]. It is found that layout optimization results are extremely sensitive to the wind condition employed for the optimal design, which is hard to be predicted accurately in real world [13]. Besides, the natural characteristics of wind speed/direction variations can

* Corresponding author. Department of Mechanical Engineering, University of Alberta, Edmonton, Alberta, T6G 1H9, Canada.
E-mail address: ming.zuo@ualberta.ca (M.J. Zuo).

https://doi.org/10.1016/j.energy.2019.116149
0360-5442/

impose additional adverse impact on the effectiveness of wind farm layout optimization design result in large wind power variability which leads to an increased operational costs of electrical systems to balance the wind power fluctuations [14]. It has been pointed out that only maximizing the average output is inadequate, as the layout design optimized in terms of the highest average power output does not necessarily guarantee results in the lowest variability of the power output, while the variability of power output from wind farm is a major concern for the power grid.

Among the wind farm layout optimizations reported in literature, a small number of researchers have incorporated the factor of wind condition unpredictability/uncertainty into their research. Gaumond et al. [15] considered the wind direction uncertainty to correct the commonly used simplified wake models in optimization study. MirHassani and Yarahmadi [16] conducted an wind farm optimization by accommodating the optimization model by incorporating uncertainty parameters into the wind characteristics. Afanasyeva et al. [17] conducted an optimization of wind farm layout with the objective function of annual energy production. The probability distribution is obtained by incorporating uncertainties of the wind speed, wind direction, wind turbine power curve and wind farm net present value. Song et al. [18] divided a 24-h day into two partitions with different parameters of the Weibull distribution wind speed model to consider the wind speed variation at different times of the day. A two-stage optimization framework is proposed to optimize the number of wind turbines and their placements by genetic algorithm and pattern search algorithm. The optimization objective is to maximize the wind energy profit, which is calculated as the energy production revenue subtracted by the capital and maintenance cost. Padron et al. [19] proposed a polynomial chaos method to efficiently quantify the variation of annual energy production of a wind farm by considering the uncertainty of wind speed and wind direction with the objective of annual energy production. A more accurate optimization result is obtained with less computational cost consumption compared to that with the commonly used simplistic integration technique. Messac et al. [20] performed a robust wind farm layout optimization by introducing the wind resource-based uncertainty, and both the annual energy production and the cost of energy production are optimized in the research. The optimization results in the work illustrated the importance of reducing the sensitivity of layout design to the actual wind condition. From the existing research work on wind farm design only a small number has incorporated the wind power variance/variability as the optimization objective function and it needs to be addressed.

For the topic of wind power variability, the existing research work mainly focused on quantification methods of wind power variation and subsequent operational measures of mitigating the wind power fluctuations [21,22]. Boutsika and Santoso [23] proposed a conditional range metric to be applied for quantifying short-term wind power variability, which is essential for the power system operators to determine the operating reserve requirements of wind power. Sorensen et al. [24] tested a wind power fluctuation model for the Horns Rev offshore wind farm, and it shows a reasonable agreement between the simulation and measurement results of ramping characteristics at different power levels and the need for system generation reserves due to fluctuations. Holttinen et al. [25,26] applied standard deviation of hourly variation as an indicator of wind power variability to measure the operational reserve requirement for wind power caused by the fluctuating characteristics. Nevertheless, the research on wind farm layout optimization with the inclusion of wind power variability has not been reported in literature. Therefore, it is worthwhile to investigate wind farm design from the beginning to mitigate wind power fluctuation prior to setting up wind farm operation.

In this paper, the wind farm power variance is employed as an indicator of the total wind power variability and the aim to optimize wind farm layout by trading off the average power output and power variance with two different single-objective optimization methods. Although there are two optimization parts involving the objective function, essentially it is still regarded as the single objective optimization problem. The Monte Carlo simulation of wind distribution is carried out to generate the discrete wind speed and wind direction bins mimicking the realistic collected wind condition data for the optimization study. The remainder of this paper is organized as follows. Section 2 describes the modelling and methodology applied in the wind farm optimization study. Section 3 presents the new proposed optimization models and the optimization algorithm. Section 4 discusses the optimization results and Section 5 concludes the research of this paper work.

2. Modelling and methodology

The PARK wake model to be described in Section 2.1 will be used in our layout optimization model with wake effects from random wind speed and random wind directions. In Section 2.2, the wind farm models that will be used in this paper are introduced. The statistical measures of wind farm power output are presented in Section 2.3, as well as the Monte Carlo method is shown in Section 2.4. The new contributions of this work is given in Section 3 together with new layout optimization models taking into consideration both the wind power output and power output variability.

2.1. PARK wake model [27]

Among the wind farm layout design study in literature, a number of simplified wake models have been applied including Larsen model [28] and Frandsen model [29]. In this paper, a simplified wake model named PARK model (see Fig. 1) is employed to quantify the wake effect between wind turbines since it consumes less computational resources with satisfying accuracy [30,31].

In the PARK model, the wake after the upstream wind turbine rotor is assumed to be linearly propagated [32]. The wake-affected wind speed is given by:

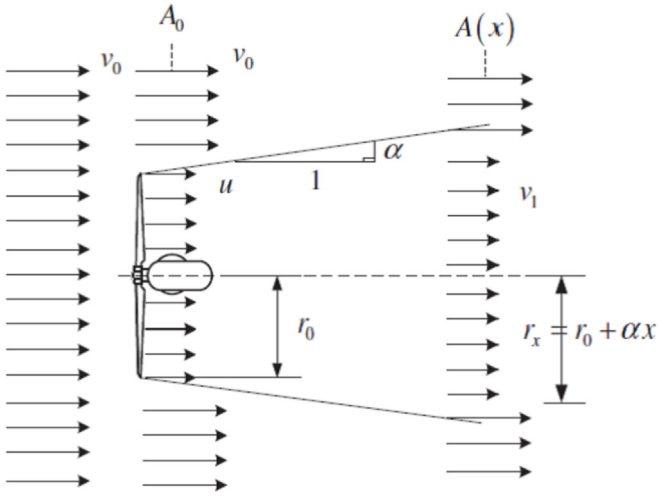

Fig. 1. Diagram of PARK wake model (linear propagation of air flow in the axial direction of the wake).

$$v_1 = v_0\left[1 - 2a\left(\frac{r_0}{r_0 + \alpha x}\right)^2\right] \tag{1}$$

where a is the axial induction factor, and r_0 is the downstream rotor radius which is given by (R is the rotor radius):

$$r_0 = R\sqrt{\frac{1-a}{1-2a}} \tag{2}$$

For sole wake interaction, the wind speed deficit (calculated as the percentage of wind speed reduction) is given by:

$$Deficit = 2a\left(\frac{r_0}{r_0 + \alpha x}\right)^2\sqrt{\frac{A_{\text{overlap}}}{A_{\text{rotor}}}} \tag{3}$$

where A_{overlap} is the overlapped area of wake radius and rotor radius (see Fig. 2 for shadowed area). When fully in the wake region, the overlapped area is the rotor area A_{rotor}. When there is no wake interaction, the area is zero.

The wind speed deficit of i-th wind turbine under multi-wake interactions is mathematically formulated by:

$$Deficit^i = \sqrt{\sum_{i=1}^{N}\left(2a\left(\frac{r_0}{r_0 + \alpha x}\right)^2\sqrt{\frac{A^i_{overlap}}{A^i_{overlap}}}\right)^2}, \quad i = 1, 2, \ldots, N \tag{4}$$

Under Weibull distribution wind condition, it is reported the scale parameter will be influenced by the wake effect and it obeys the function reported in Ref. [33]:

$$c_i = c\left(1 - Deficit^i\right), \qquad i = 1,\ 2,\ \ldots,\ N \tag{5}$$

where c_i is the resultant scale parameter under wake effect.

2.2. Wind farm models

In this section, the wind turbine model and wind condition model reported in Ref. [34] will be used in our study. The wind farm model studied in this paper is square shape and its dimensions are shown in Fig. 3. This wind farm model has been extensively studied in literature which is regarded as a benchmark model for other wind farm design research [35,36].

For the consistency of research making use of this wind farm model, the same wind turbine model reported in the literature will be used with the properties shown in Table 1. Properties of the wind turbine model for the wind farm layout [37], and a symbolic number of wind turbines (38 wind turbines) are assumed for the optimization study.

Instead of using simplistic wind conditions with discrete wind speed descriptions reported in Ref. [38], the wind speed variation represented by Weibull distribution reported in Ref. [39] is used in this paper. Its probability density function (PDF) obeys the mathematical formula of reference [40]:

$$p(v) = \frac{k}{c}\left(\frac{v}{c}\right)^{k-1}\exp\left(-\left(\frac{v}{c}\right)^k\right) \tag{6}$$

in which $p(v)$ is the probability density at a specific wind speed v, and c and k are the scale and shape parameters, respectively. In this paper, constant scale parameter of 9 and constant shape parameter of 2 for Weibull distribution are set for the optimization task. Two predominant wind directions (0° and 90°) with equal probability of 50% are assumed to be the wind direction scenario in this paper.

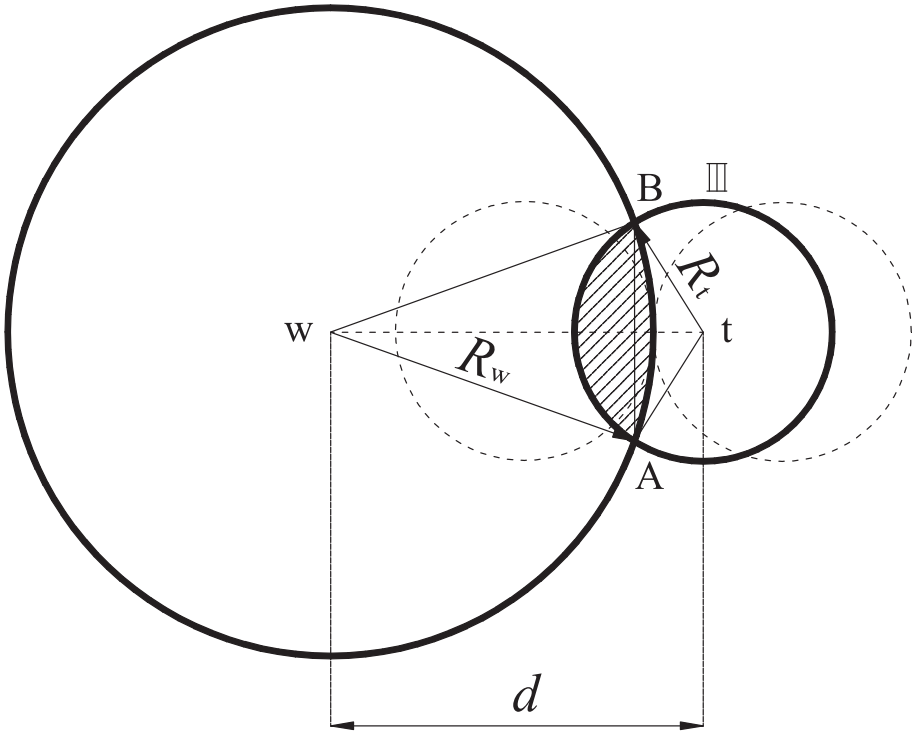

Fig. 2. Different overlapping situations of wind turbine rotor radius and wake radius (the dashed circles are the critical full-wake and free-of-wake conditions respectively, and the shadowed area is the overlapping area to be calculated).

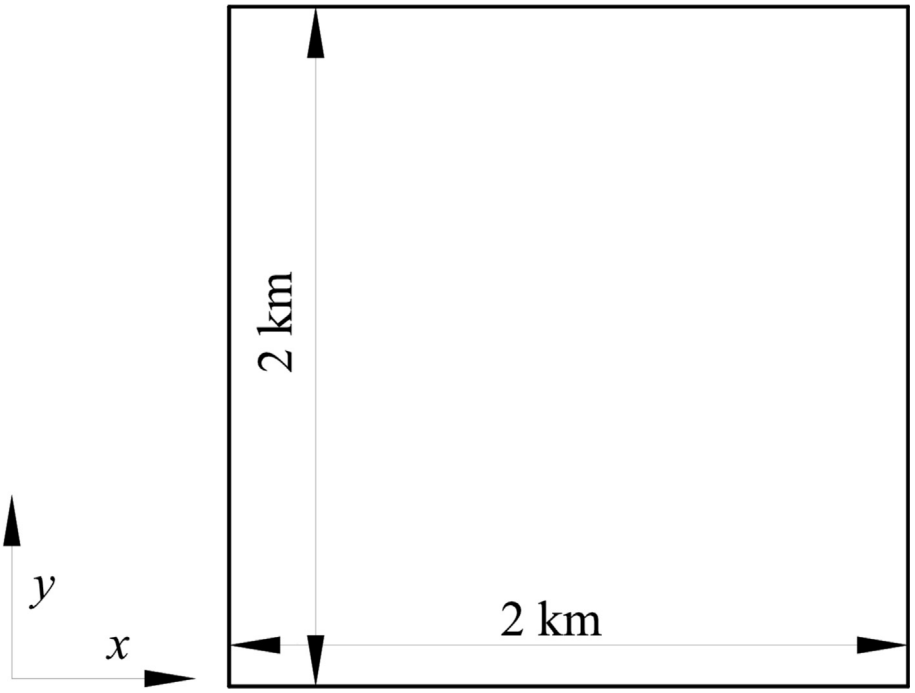

Fig. 3. Ideal square shape wind farm model in two-dimensional Cartesian coordinate system with 2 km by 2 km dimensions.

Table 1
Properties of the wind turbine model for the wind farm layout optimization study (key parameters include rated power output of 630 kW, rotor diameter of 40 m, hub height of 60 m etc.).

Parameters	Values
Rated power	630 kW
Rotor diameter	40 m
Default hub height	60 m
Cut-in wind speed	2.3 m/s
Rated wind speed	12.8 m/s
Cut-out wind speed	18 m/s
Power coefficient	0.59

2.3. Statistical measures of wind farm power output

The total power is the aggregated value of all separate wind turbine power. It is a function of wind turbine power curve, wind speed/direction, wind turbine location and others [41,42]. For a given wind farm, the wind turbine model is fixed in most cases and hence the wind turbine power curve is assumed unchanged. Thereby, the expression of a wind farm power output is given by: $P_{total} = f(v, \theta, x, y)$. In the expression, x and y indicate the wind turbine locations which are the decision variables to be determined in our research.

Due to the randomness of wind condition, both the wind speed v and the wind direction θ are stochastic. It is widely known that prediction of meteorological data of a given site, such as the magnitude and direction of the wind, cannot be accurately predicted even with advanced technologic tool. Because of the uncertainties in the wind speed and wind direction, the actual wind farm power output is a random variable in practise. In order to increase the robustness of the wind farm layout optimization it is essential to take into account wind uncertainty and utilize multiple measures including both the mean wind farm power output and the variance of wind farm power output. The mean (or average) power output indicates the expected power output of random variable wind farm power output. The variance of wind farm power output measures the dispersion of the possible random wind farm power output variable around the expected value. We can evaluate the mean and the variance of this power output random variable using Monte Carlo method to be introduced next.

2.4. Monte Carlo simulation procedure for power evaluation as a random variable

When calculating the wind turbine power, the discretization method with artificially divided wind speed and wind direction bins, is inapplicable for the wind power variability study to consider the realistic wind variations in this paper [43]. Given the randomness of wind speed and direction change in nature, Monte Carlo (MC) simulation is performed to generate the random discrete wind data and to calculate the power output and variance [44]. The detail of MC simulation is as bellow:

1. Generating random [0, 1] variable array ($\delta_i,\ i = 1, 2, \ldots, S$) is obtained with the variables uniformly distributed.
2. Simulation of the wind speed data and convert the random variables δ_i to variables X_i by performing the inverse cumulative distribution function, $X_i = F^{-1}(\delta_i)$.
3. Evaluate the accuracy of the wind speed prediction by using index of Root Mean Square Error (RMSE) to measure the difference of probability of occurrence predicted by MC simulation and the actual Weibull distribution, which is given by:

$$\mathrm{RMSE} = \sqrt{\frac{1}{N_{\mathrm{Bins}} - 1} \sum_{i=1}^{N_{\mathrm{Bins}}} \left(\phi_i(\mathrm{Bin}) - \phi_i(\mathrm{Interval})\right)^2} \tag{7}$$

where N_{Bins} is the number of total bins that the whole region is divided into. $\phi_i(\mathrm{Bin})$ and $\phi_i(\mathrm{Weibull})$ are probabilities of wind speed for the i-th simulation bin and the i-th Weibull distribution wind speed interval, respectively. From Fig. 4, $\phi_i(\mathrm{Bin})$ is calculated as the product of height and width of the histogram bin, while

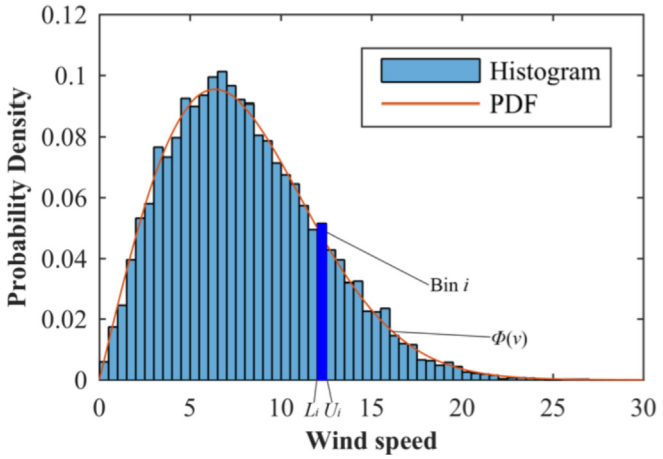

Fig. 4. Schematic of the Monte Carlo method for approximating the Weibull distribution wind condition (red line is the theoretical probability density function curve, and histogram is the simulated wind speed bins by MC method).

ϕ_i(Weibull) is calculated as the integral of probability density function curve for the given wind speed interval. They are mathematically represented by:

$$\phi_i(\text{Bin}) = height_i(\text{Bin}) \times width_i(\text{Bin}) \tag{8}$$

$$\phi_i\left(\text{Weibull}\left(= \int_{L_i}^{U_i} \phi(v) \right.\right. \tag{9}$$

4. For the simulation of wind direction data, firstly, assuming the probability from different wind direction sectors is $[p_1, p_2, \ldots, p_{N_\theta}]$. Its cumulative distribution function is given by: $P_k = \sum_{j=1}^{k} p_j$, $k = 1, 2, \ldots, N_\theta$. Likewise, create a random [0, 1] variable array $(\Delta_i,\ i = 1, 2, \ldots,\ S)$ and compare the value of P_k and Δ_i. The largest k satisfying $P_k \le \Delta_i$, is the exact random wind direction index for the task.
5. With the discrete wind speed and direction data available, the individual power and its variance can be obtained by incorporating different optimization models shown below. For j-th wind turbine, they are given by:

$$P_i(j) = \begin{cases} 0 & if\ v < 2.3\ m/s\ or\ v > 18\ m/s \\ 0.3v_i^3 & if\ 2.3\ m/s \le v < 12.8\ m/s \\ 630 & if\ 12.8\ m/s \le v \le 18\ m/s \end{cases} \tag{10}$$

$$\sigma^2(j) = \frac{1}{S-1} \sum_{i=1}^{S} \left(P_i(j) - \frac{\sum_{i=1}^{S} P_i(j)}{S} \right)^2 \tag{11}$$

The total power output of a wind farm is the summation of all power outputs of individual wind turbines. This total power output is a random variable. The average of this total power output is the sum of the averages of individual turbine power output and the variance of the wind farm total power output is the sum of the power output variances of individual turbine and is given by, $E(X) = \sum_{j=1}^{N} \sum_{i=1}^{S} P_i(j)$ and $\sigma^2(X) = \sum_{j=1}^{N} \sigma^2(j)$. Here, X is the potential wind farm layout solution with Cartesian coordinates of all wind turbines by $X = x_1 y_1 x_2 y_2, \ldots, x_n y_n$.

3. The proposed optimization models and algorithm

Instead of solely employing the energy production as the objective function for wind farm layout optimization, both the mean wind farm power output and its variability are considered for the optimization study in this paper. This unique academic contribution incorporates wind farm power output variability into layout optimization study.

For the wind farm layout optimization problem in this paper, the sole objective is to reach the trade-off between the total wind farm power output and its variance. For an optimum trade-off, the average power output should be maximized while the power output variability should be minimized, which leads to the expression of a single objective optimization problem:

$$\text{Trade} - \text{off between } E(X) \text{ and } \sigma^2(X) \tag{12}$$

$$s.t.:\ \sqrt{(x_i - x_j)^2 + \left(y_i - y_j\right)^2} \ge d_{\min}\ \forall\ i,\ \forall\ j \in n$$

$$0 \le x_i \le 2000,\ \ 0 \le x_j \le 2000 \quad \forall\ i,\ \forall\ j \in n$$

$$0 \le y_i \le 2000,\ 0 \le y_j \le 2000\ \forall\ i,\ \forall\ j \in n$$

where x and y are stored Cartesian coordinates of wind turbines, and $x_1 y_1 x_2 y_2, \ldots, x_n y_n$, which is the optimization solution consisting of all wind turbine Cartesian coordinates. d_{min} is the minimal allowable distance between any two wind turbines, which is to prevent wake effect and other catastrophic consequence if the wind turbines fall down [45]. In this paper, it is set to be 5 times of the wind turbine rotor diameter and n is the set of wind turbine number indices. The proximity constraint (first *s.t.* equation) and boundary constraint (second and third *s.t.* equations) are imposed on the objective function for optimization.

In order to trade off the wind farm power output and variance in layout optimization, two different approaches are adopted, i.e., the weighted optimization and the confidence interval (CI) optimization.

3.1. Weighted optimization

Among all different approaches to solving the optimization problem with various objective parts such as, the epsilon-constraint method and the normal boundary intersection method, the weighted method is the most popular and is also the easiest to use. Its principle to optimize different objective parts is by converting it to single objective by adding weights which indicate the importance of different objectives. In this paper, in order to investigate the trade-off of average wind farm power output $(E(X))$ and power variance $(\sigma^2(X))$, the weight parameter (α) with different values is used to quantify the proportion of these two objectives in the final optimization objective function. To equalize the magnitude of the two objective parts, the square root of power variance is implemented and the final objective function of the weighted optimization method is given by:

$$\min: f(X) = -1 \times \alpha \times E(X) + (1 - \alpha) \times \sqrt{\sigma^2(X)}\ \forall\ \alpha \in [0, 1] \tag{13}$$

the optimization objective function is the power output variance when α equals 0, and it is the average power output when α equals 1. In the equation, a weighted sum of the objectives is optimized which is easy to be solved by applying the single objective

optimization algorithm.

For the weighted optimization, one of the most important problems is the determination of the weight values for different objectives. The problem arises naturally when the importance of different objectives is hard to be quantitatively obtained. In this paper, simple linear weight constraint is considered which linearly combines the two objectives. Weight value from 0 to 1 with an increment of 0.2 is adopted to investigate the trade-off between the two objectives. One particular feature of the weighted optimization is that the objective function does not exhibit an explicit mathematical meaning except at the two extreme points with α equal to 0 and 1. With this specific optimization approach, the wind power variability (indicated by the power variance) is studied.

3.2. Confidence interval optimization

Regarding the confidence interval optimization, the idea from Ref. [21] on wind speed variability are analyzed. According to the discrete wind speed dataset, the average wind speed magnitude with 95% confidence (the confidence interval, CI) is calculated by:

$$\mu_v \pm 1.96 \times \frac{\sigma_v}{\sqrt{S}} \tag{14}$$

where μ_v is the average expected wind speed, σ_v is the standard deviation of wind speed calculated from the wind speed data of MC simulation and S is the sample number of MC simulation. With the sample number set at 10000 in this paper, the CI of wind speed is calculated to be 8±0.08 m/s. In the equation of CI definition, the second term is called the margin of error (MoE).

With CI as the average wind speed, the mean wind farm power output with 95% confidence can be formulated and the CI optimization objective is to maximize the lower end of power output CI or to minimize the upper end of power output CI given as follows:

$$\text{maximize}: \ f(X) = E(X) - 1.96 \times \sqrt{\frac{\sigma^2(X)}{S}} \tag{15}$$

$$\text{or minimize}: \ f(X) = E(X) + 1.96 \times \sqrt{\frac{\sigma^2(X)}{S}} \tag{16}$$

where $E(X)$ and $\sigma^2(X)$ are the mean wind farm power output and power variance calculated from the individual power output relating to the discrete wind speed/direction dataset, respectively. By introducing the CI of mean wind farm power output, the two objectives for the wind farm layout optimization, that is, the mean wind farm power output and variance, are integrated into one meaningful optimization target which incorporates the wind speed uncertainty to the prediction of wind farm power output. Maximizing the lower end of wind farm power output equals to both maximize the mean power output and minimize the mean power output confidence interval at the same time, which conforms to our two optimization objectives perfectly. In comparison, minimizing the upper end of wind farm power output leads to a minimization of mean power output interval which simultaneously minimizes the mean power output. Though the minimization results may not fully satisfy our optimization goals, it still can be regarded as a trade-off between the mean wind farm power output and its variance and can be used for the comparative study with maximization results.

3.3. Optimization algorithm

Based on the objective function and constraint formulation stated above, the final optimization process is to minimize the function represented by:

$$F(X) = f(X) + \psi \times (N_{WT}) \tag{17}$$

where N_{WT} is the number of wind turbines that dissatisfy the wind turbine proximity constraint and boundary constraint indicated above. The penalty method is applied for the constrained optimization study and ψ is the penalty parameter which is set to be 500. As can be seen, the value of wind turbine number that dissatisfy the proximity constraint of the minimal distance requirement is amplified by the penalty parameter, and then added to the objective function leading the whole optimization process to search for the feasible solutions.

In this paper, the single objective genetic algorithm (SOGA) is employed as the optimization algorithm for the wind farm layout optimization study. SOGA is a metaheuristic algorithm that mimics the process of natural selection which is under the category of evolutionary algorithm (EA). The algorithm searches the variable domain relying on the bio-inspired operators such as mutation, crossover and selection [46]. The main principle of SOGA is the evolvement of encoded solutions guided towards the optimum step by step iteratively. Fig. 5 shows the steps for the evolved optimization solutions which are repeated until the stopping criterion (maximum generation number) is met [47]. In the optimization, the size of population is set to 100 with 76 optimization variables (coordinates of 38 wind turbines).

It begins with the fitness evaluation of the initial population, followed by the selection of elite solutions and the parent solutions for mating to produce offspring solutions by crossover and mutation operations. The selected elite and offspring solutions form the new population. Their fitness is further evaluated and the above

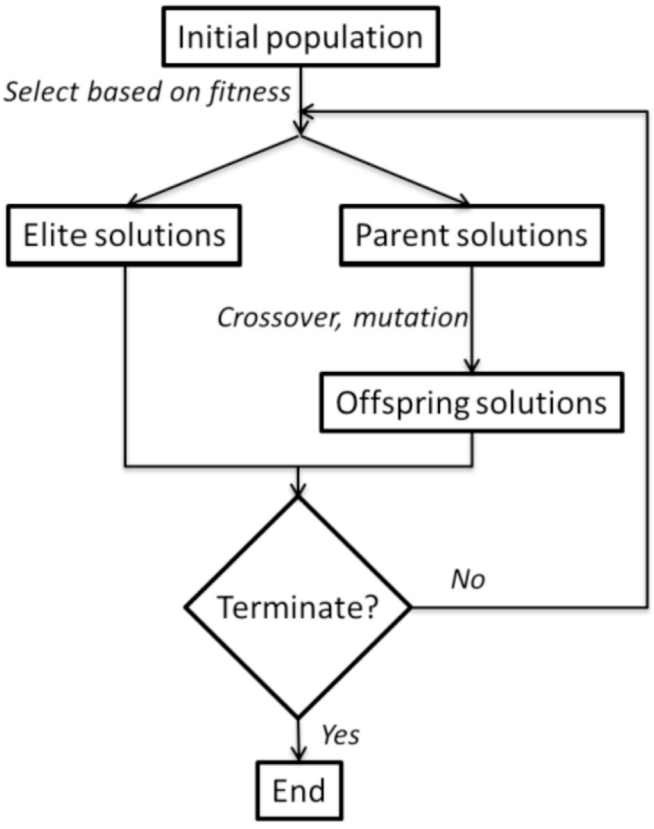

Fig. 5. Flowchart of the single objective genetic algorithm (SOGA) principle.

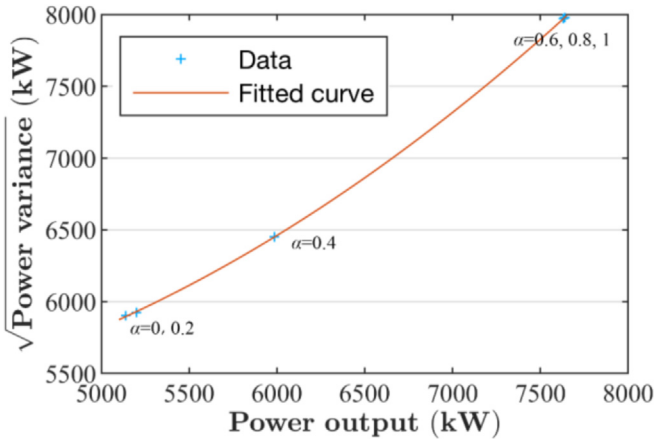

Fig. 6. Trade-off between the total wind farm power output and power variance under equally predominant wind directions of 0° and 90°, where square root of power variance is employed to balance the quantity of the power output and its variance.

procedures are repeated until the stopping criterion is met.

4. Results and discussion

In this paper, two predominant wind directions of 0° and 90° with equal probability and the Weibull distribution wind speed variation are employed as the wind condition. For a scenario with 38 wind turbines, optimization of the wind farm layout with variable power output is performed in this study. The Root Mean Square Error (RMSE) value of the MC simulation is calculated to be 0.12% (relative to the probability range of [0, 1]), which proves a good fit of the MC approximation on the original Weibull distribution. For the whole simulation/optimization study, the computation platform with two 64-bit Intel Xeon Cores and 2 Gigabytes memory running on SUSE Linux operating system is established. MC simulation is conducted using Matlab software and only needs to run once to generate the discrete wind speed/direction dataset which is subsequently read by the wind farm optimization codes. Optimization codes are programmed by C++ language including the standard GA codes and the fitness evaluation codes etc., which are compiled by Intel compiler for iterative calculation.

4.1. Trade-off by weighted optimization

First, the results of trading off the average power output and power variance by the weighted optimization approach are presented. Fig. 6 shows the trade-off between the total wind farm power output and power variance as a function of the weight value. As the α value increases, both the total power output and power variance increase up to $\alpha = 0.6$. The square root of power variance is employed to balance the quantity of the power output and its variance)As the weight value further increases, the wind farm yields almost the same total power output and power variance. The variations of individual wind turbine power output and the wind farm efficiency as a function of the weight value are presented in Fig. 7. Notice that the individual wind turbine power output is arranged in the increasing order to better display the comparative result of power output variation. Evidently, the power obtained with a smaller α value (up to 0.4) is much less than those with a larger α value. The individual wind turbine power obtained by an α value larger than 0.6 are approximately the same, while the discrepancy of power output for different wind turbines is very small. When $\alpha = 0.4$, it yields a much smaller power output for most of the wind turbines. In comparison, the individual wind turbine power output with $\alpha = 0.2$ are slightly larger than those with $\alpha = 0$. By observing the variation of wind farm efficiency, it is also found that the efficiency generally increases as the value of α gets larger. However, when α value is above 0.6, the an efficiencies are almost constant.

The optimal wind farm layouts obtained by the optimization of different weight values are presented in Fig. 8. The indices of the wind turbines are marked in the order of increasing individual power production as shown in Fig. 7 (a). As can be seen, the wind turbine distribution shows an aligned pattern when α is smaller than 0.4, which is beneficial to reduce the power variance. When $\alpha = 0.4$, the wind turbine positions become slightly disorganized. When α increases to 0.6, the wind turbines exhibit a staggered distribution pattern which is totally different from that with a smaller α value. When α is larger than 0.6, more wind turbines are placed to avoid the wake interactions and they are staggered along both 0° and 90° wind directions.

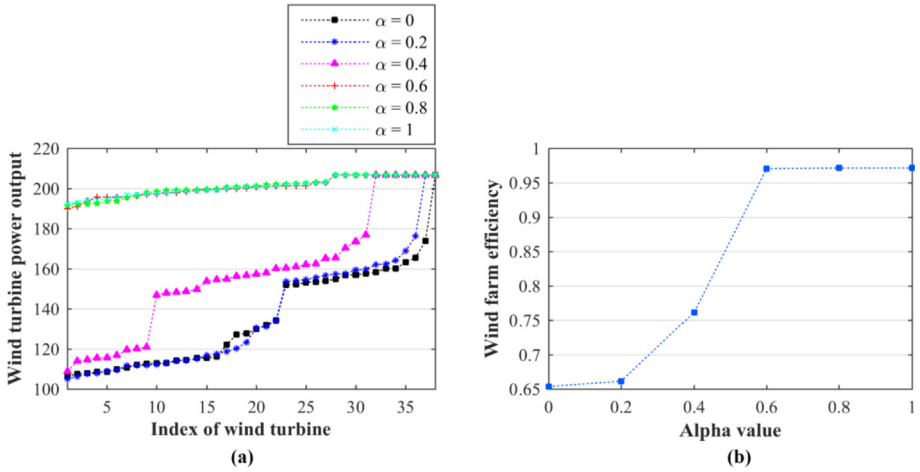

Fig. 7. Wind farm optimization results under equally predominant wind directions of 0° and 90°: (a) individual wind turbine power output for different α values and (b) wind farm efficiency as a function of weight value α.

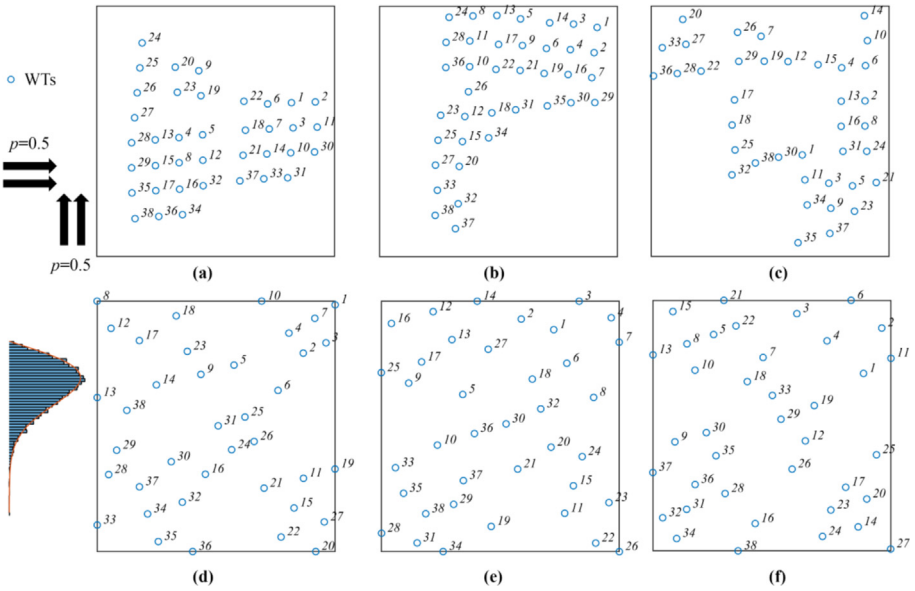

Fig. 8. Optimal wind farm layouts for different weight values: (a) $\alpha = 0$, (b) $\alpha = 0.2$, (c) $\alpha = 0.4$, (d) $\alpha = 0.6$, (e) $\alpha = 0.8$ and (f) $\alpha = 1$ (wind turbine indices are marked in the order of increasing power output shown in Fig. 7).

4.2. Trade-off by confidence interval (CI) optimization

Next, the results of CI optimization approach are presented. Firstly, the mean wind farm power output and the power output variance obtained from the maximization of lower end CI and the minimization of upper end CI are presented in Fig. 9. As can be seen, by maximizing the lower end of wind farm power output CI, the average total power output is approximately 7600 kW while the square root of total power output variance is close to 8000 kW. In comparison, the results obtained from minimizing the upper end of wind farm power output CI are much smaller. The average total power output is approximately 5000 kW while the square root of power output variance is about 5800 kW. The distribution of random wind farm power output variable for maximizing/minimizing the total power output CI are presented in Fig. 10. Evidently, the maximization study does not only reduces the chance of producing smallest wind farm power output, but also boosts the probability of achieving largest wind farm yield. By comparing to the study of minimizing the CI, the maximization study obtains a higher average power output with a slightly larger average power output interval.

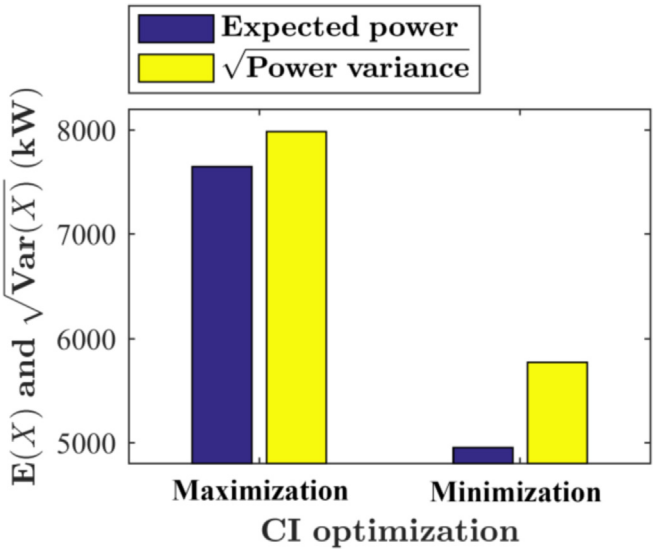

Fig. 9. Expected/mean wind farm power output and square root of power variance for both lower bound maximization and upper bound minimization of CI optimization method. Obviously the discrepancy of the maximization and minimization results is relatively large while the expected power output is slightly less than the square root of power variance.

Fig. 11 shows the individual wind turbine power output and power loss with the respective margin of error (MoE) optimized by maximizing the lower end of power output CI, and they are arranged in a monotonously increasing/decreasing order. As shown in Fig. 8, note that with 95% confidence the wind farm yields a total power output of about 7600 kW. Individually, each wind turbine has a different power output and loss. The least-produced wind turbine yields a power output of 192 kW while the power loss is as much as 15 kW. In comparison, when there are 12 wind turbines achieving a theoretically maximum power output of 207 kW without any power loss. The MoE for power output is almost constant with approximately 8–9 kW, while the MoE for power loss generally decreases with more power output produced. Fig. 12 shows the optimal wind farm layout obtained from the CI lower end maximization with the wind turbine indices indicated in the same order of increasing power output as in Fig. 11. Since the two dominant wind directions are perpendicular to the wind farm sides which have equal probability of occurrence, all wind turbines are staggered along the incoming two directions. They are spread all over the region to fully take the advantage of the broadness of the wind farm area so as to alleviate the wake effect by increasing the distances of wind turbines placement apart from each other.

The individual wind turbine power output and power losses optimized by minimizing the upper end of power output CI are shown in Fig. 13, as well as the optimal wind farm layout is shown in Fig. 14. In comparison to the maximization study, both the individual wind turbine power output and its MoE are much smaller. The least-produced wind turbine yields a power output of approximately 105 kW with a power loss close to 100 kW. However, there is only one wind turbine that is able to escape from the wake effect and generate the maximum 207 kW with no wake loss. The

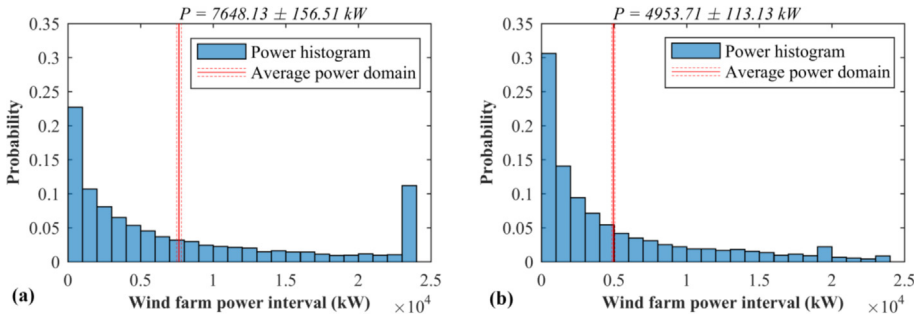

Fig. 10. Distribution of random wind farm power output variable with the mean power output value and its margin of error for the CI optimization: (a) lower bound maximization and (b) upper bound minimization. The maximization power output is larger than the minimization power output both for the average value and its domain.

distribution of optimal wind turbine locations obtained from minimizing the upper end of power output CI is obviously distinct from that with maximization study. As can be seen, all wind turbines are aligned with each other and gathered around the central part of the wind farm area. In this manner, the wind turbine wake losses increases with a much less total power output variance.

4.3. Comparison between weighted optimization and CI optimization

Finally, the optimization results of the two approaches are compared to shed light on their effectiveness on trading off the mean power output and power variance for wind farm layout optimization.

The wind farm layout optimization results with the two optimization approaches are compared in Table 2 in a quantitative manner. By observing the wind farm results, it is found the maximization of CI with lower end achieves a very close trade-off of total wind farm power output (7648 kW) and square root of power variance (7985 kW) to the weighted optimization with α value equal to or more than 0.6, implying that the proportion of average total power output on the objective function is higher than the power output variance by maximizing the CI. Except for the wind farm power output results, the range of individual turbine power output for the two optimization approaches is exactly the same and they both yield an individual power output between 192 kW and 207 kW. The total wind farm power and its variance results for the minimization of CI with upper end and the weighted optimization with α value less than or equal to 0.4 are also close to each other, but in general, their discrepancy is slightly larger. They also have the same individual wind turbine power output range, which is expected. The optimal wind farm layouts obtained by the CI maximization and the weighted optimization with α value equal to or more than 0.6, are similar to those with staggered wind turbine distribution pattern, while the optimal wind farm layouts for the other two scenarios are aligned. In addition to the optimization results, the computational costs of the two optimization approaches are also compared which are quantified by the wall time of running on High Performance Computer (HPC). It is found that with a total of 100000 generations evolved, the average

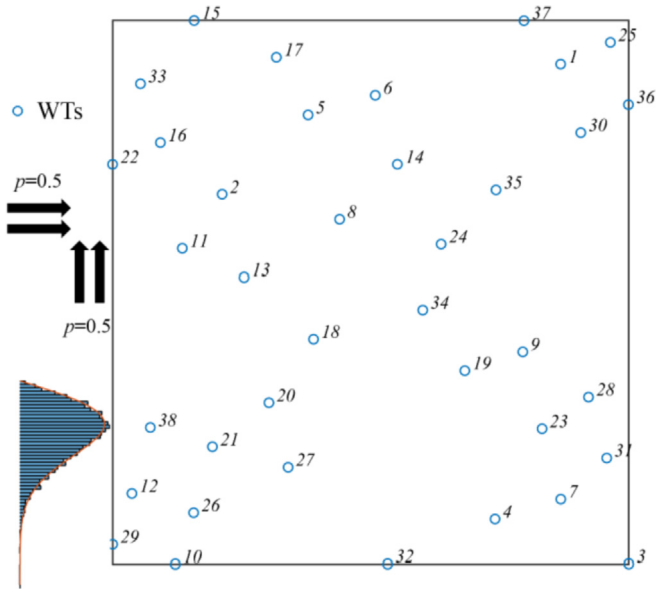

Fig. 12. Optimal wind farm layout from maximizing the lower bound of CI (wind turbine indices are marked in the order of increasing power output as in Fig. 10). Generally speaking, the optimal wind turbine placements show a staggered pattern.

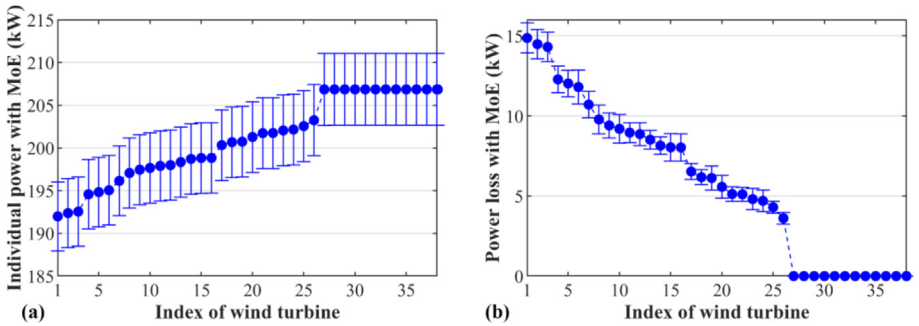

Fig. 11. Individual wind turbine optimization results from maximizing the lower bound of CI: (a) individual power output with margin of error (MoE) and (b) individual power loss with margin of error (MoE).

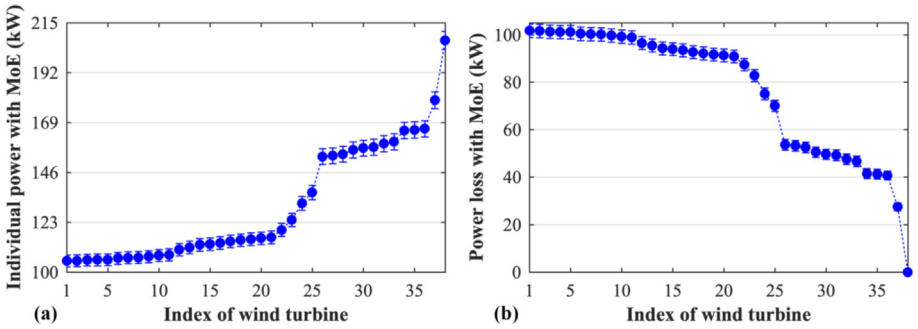

Fig. 13. Individual wind turbine optimization results from minimizing the upper bound of CI: (a) individual power output with margin of error (MoE) and (b) individual power loss with margin of error (MoE).

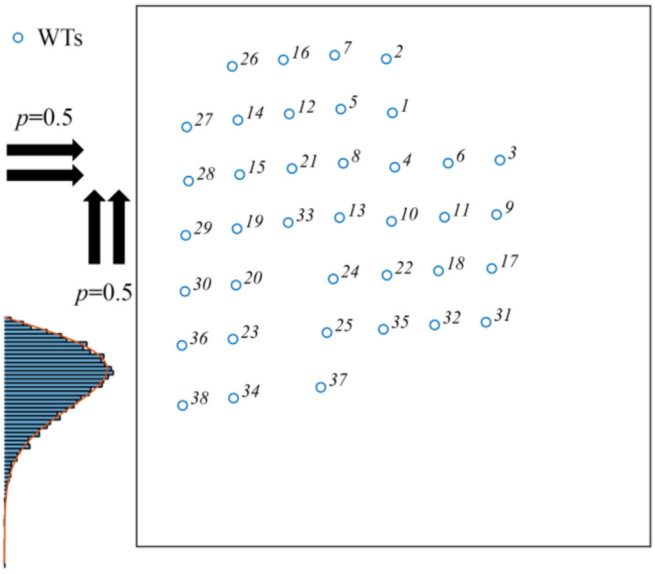

Fig. 14. Optimal wind farm layout from minimizing the upper bound of CI (wind turbine indices are marked in the order of increasing power output as in Fig. 12). Generally speaking, the wind turbine placements show a aligned pattern.

computation time of weighted optimization is 4 h 30 min while is around 4 h 45 min for the CI optimization.

5. Summary and conclusion

In this paper, an innovative method is presented on optimization of wind farm layout design by considering the wind power variability (indicated by the wind power variance) as one optimization objective. The two different approaches, weighted optimization and confidence interval (CI) optimization, are compared in term of their performances on trading off the wind farm power output and power variance with the single objective genetic algorithm. For the weighted optimization, varying weight value (α) from 0 to 1 is investigated. For the CI optimization, either the lower end of the average power output interval is maximized or the upper end of the average power output interval is minimized, with both average wind farm power output and variance are incorporated into the optimization task.

For the weighted optimization approach, as the weight value, α, increases from 0 to 1 both the total power output and power variance increase up to $\alpha = 0.6$. In general, the smaller the weight value is, the less power output individual wind turbines produce. For weight value above 0.6, the discrepancy of individual wind turbine power output is extremely small. When the weight value is small (up to 0.4) the distribution of wind turbine positions shows the alignment, and it shows a staggered placements of wind turbines when the weight value is larger than 0.6. For the CI optimization, the maximization study achieves a trade-off of power output and power variance similar to the weighted optimization with $\alpha \geq 0.6$, and the optimized individual wind turbine power output for both are from 192 kW–207 kW with the staggered placements of wind turbines inside the wind farm. The margin of error for individual wind turbine power output is approximately 8–9 kW. On the other hand, the minimization of the upper end of power output CI obtains a close trade-off result of average power output and power variance to the weighted optimization with $\alpha \leq 0.6$, and the optimal wind farm layouts are both aligned.

Nevertheless, note that the wind regime studied in this paper is simplistic, based on which the conclusions made might not be applicable under more complex wind regimes. Further work is required to compare the two different approaches to trading off the power and power variance under a more realistic wind scenario. Moreover, referring to the wind tunnel or experimental study for single wind turbine [48,49], test of multiple wind turbine operation should be also considered as a possible task in the future to validate the wind farm optimization results.

Table 2
Comparison of the wind farm layout optimization results for different approaches. Evidently, the results of weighted optimization with $\alpha \leq 0.4$ are close to the CI minimization approach, while the results of weighted optimization with $\alpha \geq 0.6$ are close to the CI maximization approach.

Approaches	Results		
	Mean power output and $\sqrt{\text{power variance}}$ trade-off	Individual power output	Optimal layout distribution
Weighted optimization ($\alpha \leq 0.4$)	Less than 5985 kW and 6450 kW	105 kW–207 kW	Aligned
Weighted optimization ($\alpha \geq 0.6$)	More than 7635 kW and 7975 kW	192 kW–207 kW	Staggered
CI maximization	7648 kW and 7985 kW	192 kW–207 kW	Staggered
CI minimization	4951 kW and 5772 kW	105 kW–207 kW	Aligned

CRediT authorship contribution statement

Longyan Wang: Methodology, Investigation, Writing - original draft. **Ming J. Zuo:** Conceptualization, Writing - review & editing, Supervision. **Jian Xu:** Data curation, Validation. **Yunkai Zhou:** Data curation, Validation. **Andy C. Tan:** Writing - review & editing.

Acknowledgements

This research is funded by Australia Endeavour Scholarships and Fellowships, Future Energy Systems under Canada First Research Excellent Fund (FES-T14-P02), the China Postdoctoral Science Foundation (2018M632244), Natural Science Foundation of Jiangsu Province (BK20180879), and High-level Talent Research Foundation of Jiangsu University (18JDG012). Comments from the reviewers and the editor are very much appreciated.

References

[1] Dai H, Xie X, Xie Y, Liu J, Masui T. Green growth: the economic impacts of large-scale renewable energy development in China. Appl Energy 2016;162:435–49.
[2] Hosseini SE, Wahid MA. Hydrogen production from renewable and sustainable energy resources: promising green energy carrier for clean development. Renew Sustain Energy Rev 2016;57:850–66.
[3] Winder VL, McNew LB, Gregory AJ, Hunt LM, Wisely SM, Sandercock BK. Space use by female Greater Prairie-Chickens in response to wind energy development. Ecosphere 2014;5(1):1–17.
[4] Imholte DD, et al. An assessment of U.S. rare earth availability for supporting U.S. wind energy growth targets. Energy Policy 2018;113(November 2017):294–305.
[5] Martínez E, Latorre-Biel JI, Jiménez E, Sanz F, Blanco J. Life cycle assessment of a wind farm repowering process. Renew Sustain Energy Rev 2018;93(April):260–71.
[6] Kuo J, Rehman D, Romero DA, Amon CH. A novel wake model for wind farm design on complex terrains. J Wind Eng Ind Aerodyn 2018;174(December 2017):94–102.
[7] Christiansen MB, Hasager CB. Wake effects of large offshore wind farms identified from satellite SAR. Remote Sens Environ 2005;98(2–3):251–68.
[8] Wilson D, et al. Evolutionary computation for wind farm layout optimization. Renew Energy 2018;126:681–91.
[9] Wang L, Tan ACC, Gu Y, Yuan J. A new constraint handling method for wind farm layout optimization with lands owned by different owners. Renew Energy 2015;83:151–61.
[10] Mosetti G, Poloni C, Diviacco D. "Optimization of wind turbine positioning in large wind farms by means of a Genetic algorithm. J Wind Eng Ind Aerody 51:105–116. J Wind Eng Ind Aerodyn 1994;51(51):105–16.
[11] Rahbari O, Vafaeipour M, Fazelpour F, Feidt M, Rosen MA. Towards realistic designs of wind farm layouts: application of a novel placement selector approach. Energy Convers Manag 2014;81:242–54.
[12] Feng J, Shen WZ. Modelling wind for wind farm layout optimization using joint distribution of wind speed and wind direction. Energies 2015;8(4):3075–92.
[13] Wang L, Cholette ME, Zhou Y, Yuan J, Tan ACC, Gu Y. Effectiveness of optimized control strategy and different hub height turbines on a real wind farm optimization. Renew Energy 2018;126:819–29.
[14] Katzenstein W, Apt J. The cost of wind power variability. Energy Policy 2012;51:233–43.
[15] Gaumond M, Réthoré P-E, Ott1 APS, Bechmann A, Hansen KS. Evaluation of the wind direction uncertainty and its impact on wake modeling at the Horns Rev offshore wind farm. Wind Energy 2014;17(April 2013):1169–78.
[16] MirHassani SAA, Yarahmadi A. Wind farm layout optimization under uncertainty. Renew Energy 2017;107:288–97.
[17] Afanasyeva S, Saari J, Kukkonen S, Partanen J, Pyrhönen O. Optimization of wind farm design taking into account uncertainty in input parameters. Eur. Wind Energy Conf. Exhib. 2013;35:1–10. 2013.
[18] Song S, Li Q, Felder FA, Wang H, Coit DW. Integrated optimization of offshore wind farm layout design and turbine opportunistic condition-based maintenance. Comput Ind Eng 2018;120:288–97. March.
[19] Padrón AS, Stanley APJ, Thomas JJ, Alonso JJ, Ning A. Polynomial chaos for the computation of annual energy production in wind farm layout optimization. J Phys Conf Ser 2016;753:032021.
[20] Messac A, Chowdhury S, Zhang J. Characterizing and mitigating the wind resource-based uncertainty in farm performance. J Turbul 2012;13:N13.
[21] Feng J, Shen WZ. Wind farm power production in the changing wind: robustness quantification and layout optimization. Energy Convers Manag 2017;148:905–14.
[22] Kuo J, Romero D, Amon CH. Robust wind farm layout optimization. Adv Trends Optim Eng Appl 2017:367–75. no. June.
[23] Boutsika T, Santoso S. Quantifying short-term wind power variability using the conditional range metric. IEEE Trans Sustain Energy 2012;3(3):369–78.
[24] Sørensen P, et al. Power fluctuations from large wind farms. IEEE Trans Power Syst 2007;22(3):958–65.
[25] Holttinen H. Hourly wind power variations in the nordic countries. Wind Energy 2005;8(2):173–95.
[26] Holttinen H, Milligan M, Kirby B, Acker T, Neimane V, Molinski T. Using standard deviation as a measure of increased operational reserve requirement for wind power. Wind Eng 2008;32(4):355–77.
[27] Wang L, Tan ACC, Gu Y. Comparative study on optimizing the wind farm layout using different design methods and cost models. J Wind Eng Ind Aerodyn Nov. 2015;146:1–10.
[28] Larsen GC, Aagaard MH, Sørensen NN. Mean wake deficit in the near field. In: European wind energy Conference and exhibition. vol. 2003; 2003.
[29] Frandsen S. On the wind speed reduction in the center of large clusters of wind turbines. J Wind Eng Ind Aerodyn 1992;39(1–3):251–65.
[30] Abdelsalam AM, El-Shorbagy MA. Optimization of wind turbines siting in a wind farm using genetic algorithm based local search. Renew Energy 2018;123:748–55.
[31] Wang L, Cholette ME, Fu Y, Yuan J, Zhou Y, Tan ACC. Combined optimization of continuous wind turbine placement and variable hub height. J Wind Eng Ind Aerodyn 2018;180:136–47.
[32] Jensen NOO. A note on wind generator interaction. 1983.
[33] Lackner MA, Elkinton CNC. An Analytical Framework for Offshore Wind Farm Layout Optimization. Wind Eng. 2007;31(1):17–31.
[34] Zhenzhou Z, Siyue Q, Yuan Z. Enhancement approaches of aerodynamic performance of lift-type vertical axis wind turbine considering small angle of attack. J. Drain. Irrig. Mach. Eng. 2018;36(2):146–53.
[35] Wang L, Tan ACC, Cholette ME, Gu Y. Optimization of wind farm layout with complex land divisions. Renew Energy 2017;105:30–40.
[36] Parada L, Herrera C, Flores P, Parada V. Wind farm layout optimization using a Gaussian-based wake model. Renew Energy 2017;107:531–41.
[37] Grady SA, Hussaini MY, Abdullah MM. Placement of wind turbines using genetic algorithms. Renew Energy 2005;30(2):259–70.
[38] Wang L, Zhou Y, Xu J. Optimal irregular wind farm design for continuous placement of wind turbines with a two-dimensional jensen-Gaussian wake model. Appl Sci 2018;8(12):2660.
[39] Wang L. Comparative study of wind turbine placement methods for flat wind farm layout optimization with irregular boundary. Appl Sci 2019;9:639.
[40] Shakoor R, Hassan MY, Raheem A, Rasheed N. Wind farm layout optimization using area dimensions and definite point selection techniques. Renew Energy 2016;88:154–63.
[41] Wenju J, Jianwen W, Shuo X, Al E. Analysis of vertical axis wind turbine power changing with rotating speed from vertical and horizontal flow fields. J. Drain. Irrig. Mach. Eng. 2018;36(2):166–71.
[42] Chenguang S, Zhenzhou Z, Guoqing W, Al E. Effect of wind speed and airfoil camber on aerodynamic performance of vertical axis wind turbines. J. Drain. Irrig. Mach. Eng. 2018;36(3):243–9.
[43] Kusiak A, Song Z. Design of wind farm layout for maximum wind energy capture. Renew Energy 2010;35(3):685–94.
[44] Wang L, Yuan J, Cholette ME, Fu Y, Zhou Y, Tan AC. Comparative study of discretization method and Monte Carlo method for wind farm layout optimization under Weibull distribution. J Wind Eng Ind Aerodyn 2018;180(May):148–55.
[45] Yamani Douzi Sorkhabi S, et al. The impact of land use constraints in multi-objective energy-noise wind farm layout optimization. Renew Energy 2016;85:359–70.
[46] Contributors W. Genetic algorithm [Online]. Available: https://en.wikipedia.org/wiki/Genetic_algorithm. [Accessed 3 September 2017].
[47] Horton P, Jaboyedoff M, Obled C. Global optimization of an analog method by means of genetic algorithms. Mon Weather Rev 2017;145(4):1275–94.
[48] Kotaro T, Yan L. A wind tunnel experiment of self starting capability for straight bladed vertical. J. Drain. Irrig. Mach. Eng. 2018;36(2):136–40.
[49] Yan L, Shouyang Z, Chunming Q, Al E. PIV visualization experiment on static flow field of Savonius wind turbine. J. Drain. Irrig. Mach. Eng. 2018;36(2):159–65.